C.P. No. 1096

C.P. No. 1096

MINISTRY OF TECHNOLOGY

AERONAUTICAL RESEARCH COUNCIL

CURRENT PAPERS

Laminar Boundary-Layer Calculations compared with Measurements by Hummel

by

J. C. Cooke

Aerodynamics Dept., R.A.E., Farnborough

LONDON: HER MAJESTY'S STATIONERY OFFICE

1970

PRICE 8s 0d [40p] NET

U.D.C. 532.526.2 : 533.693.1 : 533.693.3 : 517.948.1 :
517.949.2 : 533.6.011.12

C.P. No. 1096*
September 1967

LAMINAR BOUNDARY LAYER CALCULATIONS COMPARED WITH MEASUREMENTS BY HUMMEL

by

J.C. Cooke

Aerodynamics Dept., R.A.E., Farnborough

SUMMARY

Calculations by an integral method assuming small cross-flow, and by a finite-difference method assuming the flow to be quasi-conical, are compared with measurements made available by Hummel (Technical University, Brunswick) on a highly swept delta wing at high incidence.

It is found that the small-cross-flow method gives a rough general picture of the flow but is inaccurate in the details, especially velocity profiles. For this problem the quasi-conical method is more accurate over most of the flow field and gives a much better representation of the velocity profiles.

---

* Replaces R.A.E. Technical Report 67227 - A.R.C. 29747.

CONTENTS

1 INTRODUCTION

Hummel[1] has made a series of boundary layer measurements on a triangular plate of aspect ratio 1.0 at an angle of incidence of 20.5° and a Reynolds number based on maximum chord of 9.10^{5}. At this high incidence the flow separates from the leading edges, forming the familiar coiled vortex sheets, and the flow reattaches along the centre line of the upper surface, spreads outwards and separates again along a secondary separation line. The flow was laminar and the Mach number low enough for the flow to be considered to be incompressible. In the calculations to be discussed here attention was concentrated on the upper surface.

At such a high incidence one might have expected the external flow to be conical, but in fact it was not so; though it did appear from the measurements that the external streamlines crossed each radius vector from the apex at a nearly constant angle, the velocity decreased almost linearly along them. There was thus an "unfavourable" pressure gradient along the rays. On the other hand, for most of the surface until just before the secondary separation line, the velocity increased as one moved outwards across the span, and thus the pressure distribution in this direction was "favourable" in the sense of Maskell and Weber[2]. Just before separation this became unfavourable but it was a quite sudden change.

Originally it was expected that the flow would be nearly conical and the intention was to apply the calculation method of Ref.3 to these experiments for purposes of comparison. On receipt of the measurements, however, it was seen that the method could not be directly applied, though the possibility of assuming the flow to be locally conical might be borne in mind. The method first used was that of Ref.4, which is a momentum-integral method assuming small cross-flow. Here the maximum cross-flow angle is over 20° and so the method is being stretched beyond its region of validity, which is often believed to be for a cross-flow of not more than 15°. The calculations were performed using the measured pressure distribution and external flow direction as input data.

The main test used to assess the method of calculation was the examination of the angle β_w between the limiting streamlines and the centre line. It was found that the two curves for β_w (calculated and measured) run more or less parallel to each other, with an almost constant difference of 5°.

Attempts were also made to compare the velocity profiles at two stations, but momentum-integral methods by their very nature cannot be expected to give good results for velocity profiles. In addition the measurements were such that there were very few points available near to the wall. Agreement was poor.

The conclusion from this test is that the method of Ref.4 may be possible for a quick assessment of the main properties but that it is inadequate for a detailed accurate calculation.

On the other hand, the assumption of locally conical flow leads to better results over most of the region, and the velocity profiles agreed with the measurements fairly closely.

2 THE MEASURED DATA

The coordinate system used is Cartesian, x being measured from the apex along the centre line and y normal to this line on the surface; z is normal to the plane of the wing. All are non-dimensionalized by the maximum chord c_o. In addition if $s(x)$ is the non-dimensional semi-span at any x station then we use the coordinate $\eta = y/s(x)$ instead of y. For a triangular wing we have $s(x) = Kx$ where K is a constant. The wing in question had aspect ratio 1 so that $K = \frac{1}{4}$ in this case, and each radius vector is such that η is constant along it with $\eta = \pm 1$ at the leading edges. The angle of sweep is 76°.

2.1 External flow streamlines

From the measurements the angle β_e between the external direction of flow and the centre line was plotted as shown in Fig.1, from which it will be seen that the points fall on a single curve except for some scatter in the region $0.5 < \eta < 0.7$. Scatter is likely in places where x is small owing to the difficulties of measurement, and a mean curve was drawn through the points; in the range of η just mentioned those for the larger values of x were considered more reliable.

From the measurements the equation of the external streamlines can be calculated as in Appendix A. Those actually used in the calculations are drawn in Fig.2.

2.2 Pressure distribution

Two means of finding the pressure were available from the measurements. One was by the velocity in the external stream as given by Hummel[1], and the other by the pressure coefficient as determined from pressure holes on the surface. If the pressure across the boundary layer is constant there should be no difference between the pressures obtainable by the two methods. Unfortunately they did not agree so it was decided to use the pressure obtained from the pressure holes as likely to be more reliable. Some of the measurements are shown in Fig.3. It will be seen that there is some scatter. It was necessary to do some smoothing and to make extrapolations towards $x = 0$. The latter were rather arbitrary but it is not believed that this will make much difference to the boundary layer results downstream. The final adopted pressure distribution is shown plotted in two different ways in Figs.4 and 5.

3 THE CALCULATION METHOD

3.1 Small cross-flow

This was fully described in Ref.4 and will only be summarised here. The calculation follows streamlines and the first operation is to calculate these, as described in Appendix A.

Streamline coordinates are used with lines ψ constant representing streamlines and ϕ = constant their orthogonal trajectories. ϕ is not necessarily a velocity potential or ψ a stream function. The line element ds is given by

$$ds^2 = \frac{d\phi^2}{\rho_1 V_e^2} + \frac{d\psi^2}{\rho_2 V_e^2} \quad , \qquad (1)$$

where V_e is the resultant velocity in the external flow, and ρ_1 and ρ_2 are functions to be determined from the shape of the external streamlines.

The profiles of u' and v', the components of velocity along and perpendicular to the external streamlines, are taken to be

$$\frac{u'}{V_e} = f(\zeta) - \Lambda g(\zeta) \ , \tag{2}$$

$$\frac{v'}{V_e} = \Pi h(\zeta) - M g(\zeta) \ , \tag{3}$$

where

$$c_o z = (\sigma \nu)^{\frac{1}{2}} \zeta \ ,$$

$$1 - f(\zeta) = 2g(\zeta) + e^{-\zeta^2} = \frac{2}{3\sqrt{\pi}} \zeta \, e^{-\zeta^2} + \frac{2}{\sqrt{\pi}} \int_{\zeta}^{\infty} e^{-t^2} \, dt \ , \tag{4}$$

$$h(\zeta) = \zeta \, e^{-\zeta^2} , \tag{5}$$

$$\Lambda = \rho_1^{\frac{1}{2}} \sigma V_e \frac{\partial V_e}{\partial \phi} \ , \qquad M = \frac{\sigma}{2} \frac{\rho_2^{\frac{1}{2}}}{\rho_1} \frac{\partial}{\partial \psi} (\rho_1 V_e^2) \ . \tag{6}$$

σ and Π are unknowns and are found from

$$\rho_1^{\frac{1}{2}} \frac{\partial}{\partial \phi} \left(\frac{V_e^4 \sigma}{\rho_2} \right) = 5.08 \frac{V_e^2}{\rho_2} \tag{7}$$

$$\rho_2 (\rho_1 \sigma)^{\frac{1}{2}} \frac{\partial}{\partial \phi} \left(\frac{\sigma^{\frac{1}{2}} \theta_{21}}{\rho_2} \right) = \frac{1}{V_e^2} \{ \Pi + M(0.067 \Lambda - 0.669) \} \ , \tag{8}$$

where

$$\theta_{21} = - p\Pi - mM \ , \tag{9}$$

$$\left.\begin{aligned} p &= 0.2946 + 0.0223\Lambda \\ m &= 0.02983 + 0.00380\Lambda \end{aligned}\right\} \quad . \tag{10}$$

The angle γ between external streamlines and limiting streamlines is given by

$$\tan\gamma = \frac{2.6587\Pi + M}{2 + \Lambda} \quad . \tag{11}$$

Equation (7) is solved by a quadrature, whilst (8), in virtue of (9) is a linear equation in θ_{21} or Π.

For convenience the equations are all expressed in terms of x and η and the details are given in Appendix B.

3.2 Quasi-conical flow

In the problem considered the flow is such that all external streamlines cross a given radius vector at a constant angle but the magnitude of the external velocity is not constant along a radius vector, as Figs.3 and 4 show; and so the flow is not conical. We shall assume that the flow is "locally" conical, and give the name "quasi-conical" to calculations made.

We are implying that changes along a radius vector are small compared with those normal to it, and for the small aspect ratio wing under consideration this is equivalent to the assumption of slenderness. We are not calculating the external flow on this assumption (we are using measured values) but in assuming that the flow is locally conical we are making use of the fact that the wing is slender.

The method of Ref.3 may now be used directly since the terms in the main equations of Ref.3 which depend on the external flow are K and M, where

$$K = \frac{v_e}{u_e}, \qquad M = K^2 + \frac{dK}{d\theta}$$

and u_e and v_e are the mainstream velocity components along and perpendicular to a radius vector.

K is plotted in Fig.11 as a function of $\eta (= 4 \tan \theta)$. The curve of $K - 0.85\eta = K - 3.4 \tan \theta$ was plotted and approximated by suitable polynomials in θ for three contiguous regions (chosen to have continuous derivatives at their junctions) which fitted the curve very well. The finite difference method was then run through the computer exactly as in Ref.3.

4 RESULTS

4.1 Small cross-flow

A family of external streamlines was selected, namely those of Fig.2, depending on the constant C of Appendix A and the integration was carried through to separation if it occurred, or to the trailing edge if it did not. The main result plotted was the angle between limiting streamlines and the centre line. This did not vary much for a given η over the wide range of streamlines chosen and all of the results for different streamlines were plotted in one figure. The result is seen in Fig.6. The apparent scatter represents the variation between different external streamlines. For a given one of these the points form a smooth curve and the scatter represents a number of slightly different smooth curves. Also shown in the figure are Hummel's measurements by means of an oil flow technique. Over most of the range the calculated value of β_w is too high by about 5°. Nevertheless the approximate method gives a fair qualitative picture of the flow.

An attempt was made to see if the calculation could be made to agree more closely with the experiment by starting at the point $\eta = 0.1$ taking the measured value of β_w at this point, so that the starting value of Π in equation (8) was to be that given by experiment. Thus at $x = 0.1$ we started at the point A in Fig.6 instead of the point B. This made little difference. In one or two steps the new curve through A rejoined the curve through B and then continued to follow it.

Some measured and calculated velocity profiles are shown in Figs.7 and 8. It will be seen that the measurements do not go down very deeply into the boundary layer, but that in any case the agreement is very poor. In Figs.9 and 10 are shown the values of the angle β between streamlines and the centre line at different levels in the boundary layer.

As regards the determination of the separation line, given by Hummel as being at $\eta = 0.68$, Fig.6 shows that the calculation is leading to the same

neighbourhood. However in order to obtain the position more accurately smaller steps would be required; the flow is here very sensitive to the external pressure distribution which is changing very rapidly. There is not sufficient experimental data given in this region to obtain more accurate results by reducing the step size.

4.2 Quasi-conical flow

The angle β_w for this method is also shown in Fig.6 and the values of q/q_e and β for the same two selected stations as those of Figs.7, 8, 9 and 10 are also included in these figures. Once more, and for the same reason as already given, we cannot determine the separation line very accurately, but it can be seen that the calculations are leading to the measured position.

This calculation gives results closer to those of experiment, especially as regards velocity profiles.

5 CONCLUSIONS

It will be seen that the small cross-flow momentum-integral method cannot be considered to be very satisfactory in this case where the cross-flow component is large; though it gives some idea of the overall picture, the details are poorly represented. It appears that a fully three-dimensional calculation is needed, in general.

However, for cases such as these, where the direction of external flow is nearly constant along rays and the wing is slender, it would seem that a quasi-conical calculation by finite difference methods may give useful results. It gives a better surface flow picture and a very much better representation of the velocity profiles.

Methods are now being developed for making a full three-dimensional calculation[5]. These are as yet in an early stage and the starting problem needs further work. However, in due course, this series of experiments may serve as a basis for making a further comparison.

Appendix A

THE DETERMINATION OF THE STREAMLINES

If the velocity components of the external flow along and perpendicular to a ray are u_e and v_e then the polar equation of the streamlines is

$$r \frac{d\theta}{dr} = \frac{v_e}{u_e} = f(\theta) \qquad (12)$$

where $f(\theta)$ is a function of θ only as explained in section 2.1.

We write

$$x = r \cos \theta$$

$$y = r \sin \theta = Kx\eta$$

i.e.

$$x = r \cos \theta$$

$$\eta = \frac{1}{K} \tan \theta$$

and so (12) may be written

$$\frac{dx}{x} = \frac{K(1 - K\eta f)}{f(1 + K^2 \eta^2)} d\eta \quad .$$

In the case under consideration $K = \frac{1}{4}$ and so

$$\frac{dx}{x} = \frac{4 - f\eta}{f(16 + \eta^2)} d\eta \quad . \qquad (13)$$

$f(\eta)$ is plotted in Fig.11 and we see that the initial slope of the line is 0.85 and initially $f = 0.85\,\eta$.

We find on separating out the singular part in (13)

$$\frac{dx}{x} = \left(\frac{1}{3.4\eta} - \frac{16(f/\eta) + 4.4f\eta - 13.6}{3.4f(16 + \eta^2)}\right)d\eta \ .$$

Hence we have

$$\log x = \frac{1}{3.4}\log\eta - I + \text{constant} \ ,$$

where

$$I = \int_0^\eta \frac{16(f/\eta) + 4.4f\eta - 13.6}{3.4f(16 + \eta^2)}\,d\eta \ .$$

Hence we have

$$x = A\eta^{\frac{1}{3.4}}\, e^{-I(\eta)}$$

where A is a constant. Different streamlines are obtained by giving different values to A. $I(\eta)$ was evaluated numerically.

We have

$$\eta = Cx^{3.4}\, e^{3.4\,I(\eta)} = Cx^{3.4}\, B(\eta) \ .$$

$B(\eta)$ was expressed as a polynomial of the 4th degree in η and the value of η for a given x was found by iteration with first approximation $\eta = Cx^{3.4}$. This converged rapidly. This was necessary because it was found most convenient to solve the equations taking equal steps of x, the independent variable chosen, following a streamline.

The polynomial for B used was

$$B(\eta) = 1 + 5.593\eta^3 - 6.214\eta^4 \ .$$

Appendix B

THE EQUATIONS IN TERMS OF x and η

If we use polar coordinate r, θ (r being non-dimensionalized by c_o) with the apex as origin and the centre line as initial line, and if u_e and v_e are the radial and transverse velocity components of the external flow and V_e their resultant then we have

$$\frac{v_e}{u_e} = f(\theta), \qquad V_e^2 = u_e^2 + v_e^2 .$$

The streamlines ψ = constant are given by

$$r \frac{d\theta}{dr} = \frac{v_e}{u_e} = f$$

and we write

$$\psi = - \log r + \int \frac{d\theta}{f} .$$

The orthogonal trajectories ϕ = constant are given by

$$\frac{1}{r} \frac{dr}{d\theta} = - f ,$$

and we write

$$\phi = \log r + \int f \, d\theta .$$

Now when ϕ = constant we have $dr = -f r \, d\theta$ and so

$$d\psi = - \frac{dr}{r} + \frac{d\theta}{f} = \left(f + \frac{1}{f} \right) d\theta .$$

The line element, equation (1), becomes when ϕ = constant

$$c_o^2 (ds)^2 = \frac{(d\psi)^2}{\rho_2 V_e^2} = \frac{\left(f + \frac{1}{f}\right)^2 (d\theta)^2}{\rho_2 V_e^2}$$

where s is now non-dimensionalized by c_o.

But

$$ds^2 = dr^2 + r^2 d\theta^2$$

$$= r^2(1 + f^2) d\theta^2$$

along the line ϕ = constant, and so

$$\rho_2 V_e^2 = \frac{1 + f^2}{c_o^2 f^2 r^2}$$

which determines ρ_2.

Again when ψ = constant we have $dr = r d\theta / f$ and so

$$d\phi = \frac{dr}{r} + f d\theta = \left(f + \frac{1}{f}\right) d\theta$$

and in a way similar to the above we find

$$\rho_1 V_e^2 = \frac{1 + f^2}{c_o^2 r^2},$$

which determines ρ_1.

Also

$$\Lambda = \rho_1^{\frac{1}{2}} \sigma V_e \frac{\partial V_e}{\partial \phi} = \frac{\sigma f}{c_o r (1 + f^2)^{\frac{1}{2}}} \frac{dV_e}{d\theta},$$

the differentiation being along a streamline.

But along a streamline

$$\frac{dV_e}{d\theta} = V_{er}\frac{dr}{d\theta} + V_{e\theta} = \frac{r}{f}V_{er} + V_{e\theta} \quad .$$

Hence

$$\Lambda = \frac{\sigma}{c_o r}\frac{1}{(1+f^2)^{\frac{1}{2}}}(r\,V_{er} + f\,V_{e\theta}) \quad .$$

A similar calculation leads to

$$M = \frac{\sigma}{c_o r}\frac{1}{(1+f^2)^{\frac{1}{2}}}(V_{e\theta} - rf\,V_{er}) \quad .$$

Equation (7) becomes

$$\frac{d}{d\theta}\left(\frac{\sigma}{r\,c_o}V_e^6\frac{f^2}{1+f^2}r^3\right) = \frac{5.08\,V_e^5\,r^3\,f}{(1+f^2)^{\frac{1}{2}}}$$

and if we write $V_e = V_o\,q_e$, $\Sigma = \sigma\,V_o/c_o\,r$, where V_o is a representative velocity, we have

$$\frac{d}{d\theta}\left(\Sigma\,q_e^6\,\frac{f^2}{1+f^2}\,r^3\right) = \frac{5.08\,q_e^5\,r^3\,f}{(1+f^2)^{\frac{1}{2}}} \quad ,$$

differentiation being along a streamline.

Equation (8) becomes

$$\frac{d}{d\theta}\left[\frac{\Sigma^{1/2}\,\theta_{21}\,q_e^2\,f^2\,r^{5/2}}{1+f^2}\right] = \frac{q_e\,f\,r^{5/2}}{\Sigma^{1/2}(1+f^2)^{1/2}}\,[\Pi + M\,(0.067\Lambda - 0.669)]$$

differentiation being along a streamline.

It is convenient to recast these equations in terms of η and x; we are differentiating along a streamline which is known, and we may treat either x or η as the independent variable since either is known as a function of the other. Of these we shall choose x.

We write

$$s(x) = Kx , \qquad \eta = y/Kx = (1/K) \tan\theta ,$$

where $K = \frac{1}{4}$ in the particular problem considered here.

We have

$$r^2 = x^2 + y^2 = x^2(1 + K^2 \eta^2) .$$

Along a streamline

$$dx = \frac{\partial x}{\partial r} dr + \frac{\partial x}{\partial \theta} d\theta$$

$$= \cos\theta \frac{r d\theta}{f} - r \sin\theta \, d\theta$$

$$= \frac{x d\theta}{f} [1 - K\eta f] ,$$

where f is known as a function of η.

Hence finally the equations to be solved are

$$\frac{d}{dx}\left[\frac{\Sigma q_e^6 f^2 x^3 (1 + K^2 \eta^2)^{3/2}}{1 + f^2}\right] = \frac{5.08 \, q_e^5 x^2 (1 + K^2 \eta^2)^{3/2} f^2}{(1 + f^2)^{1/2} (1 - K\eta f)} \qquad (14)$$

$$\frac{d}{dx}[\Sigma^{1/2} \theta_{21} q_e^2 f^2 x^{5/2} (1 + K^2 \eta^2)^{5/4}] = \frac{q_e f x^{3/2} (1 + K^2 \eta^2)^{5/4}}{\Sigma^{1/2} (1 + f^2)^{1/2} (1 - K\eta f)}$$

$$[\Pi + M(0.067\Lambda - 0.669)] \qquad (15)$$

where Π is related to θ_{21} by equation (9).

Λ and M are now given by

$$\Lambda = \Sigma \frac{Kx\, q_{ex}(1 - Kf\eta) + f\, q_{e\eta}(1 + K^2\eta^2)}{K(1 + f^2)^{\frac{1}{2}}} ,$$

$$M = \Sigma \frac{(1 + K^2\eta^2)\, q_{e\eta} - Kx\, q_{ex}(f + K\eta)}{K(1 + f^2)^{\frac{1}{2}}} .$$

In these equations η is known as a function of x by Appendix A. The first equation determines Σ and once this is known Λ and M are known, and then the second equation determines θ_{21} or Π. When these are solved the velocity profiles, skin friction etc. are known. See Ref.4.

The main difficulty in the solution is the singular point at the start. Thus if we write $f = 0.85\eta\, h(\eta)$ in equation (13) and $\eta = Cx^{3.4} B(\eta)$, where h and B are "well-behaved" the equation becomes

$$\frac{d}{dx}\left[\frac{\Sigma\, q_e^6}{1 + f^2} h^2 B^2 x^{9.8}(1 + K^2\eta^2)^{3/2}\right] = \frac{5.08\, q_e^5 x^{8.8}(1 + K^2\eta^2)^{3/2} B^2}{(1 + f^2)^{1/2}(1 - K\eta f)} .$$

C^2 and $(0.85)^2$ cancel.

This may be written

$$\frac{d}{dx}(ex^{9.8}) = ax^{8.8}$$

where e and a are "well-behaved", and e is to be found. Standard methods like Simpson's rule are unsuitable here owing to the high powers of x involved.

If we take $dx = h$ and integrate from the $(m - 1)^{th}$ to the m^{th} step we may write this equation, with an obvious notation

$$e_m(mh)^{9.8} - e_{m-1}[(m-1)h]^{9.8} = \int_{(m-1)h}^{mh} x^{8.8}\left[a_{m-1} + \frac{a_m - a_{m-1}}{h}(x - x_{m-1})\right]dx$$

and thus e_m can be found when e_{m-1} is known.

A basically similar technique is used for equation (15), a little more complicated because the equation is of the form

$$\frac{d}{dx}(dx^{9.3}) = (bd + c)x^{8.3},$$

where d is to be found.

SYMBOLS

c_o	maximum chord
$f(\theta), f(\eta)$	v_e/u_e
$f(\zeta), g(\zeta), h(\zeta)$	profiles given by (4) and (5)
K	tan (semi-angle at vortex) = 0.25
K	(in section 3.2) v_e/u_e
M	(in section 3.2) $(1/u_e)(\partial v_e/\partial\theta)$
m	given by (10)
p	given by (10)
q	non-dimensional resultant velocity
u, v	velocity components along and perpendicular to radius vector
u', v'	velocity components along and perpendicular to external streamlines
r	polar coordinate - distance from apex
s(x)	semi-span
x, y, z	Cartesian coordinates. Origin apex, x-axis along centre line, z-axis normal to plane
β	angle between streamline and centre line
γ	angle between external and limiting streamlines
ζ	given by $c_o\, z = (\sigma\nu)^{\frac{1}{2}}\zeta$
η	$y/s(x)$
θ	polar coordinate - angle from centre line
θ_{21}	given by (9)
Λ	given by (2) and (6)
M	given by (3) and (6)
ν	kinematic viscosity
Π	given by (3)
ρ_1, ρ_2	functions in the surface line element in streamline coordinates
σ	quantity related to boundary layer thickness
ϕ	function related to velocity potential
Ψ	function related to stream function

Subscript e refers to values in the external flow

Subscript w refers to values at the wall

REFERENCES

No.	Author	Title, etc
1	D. Hummel	Zur Umströmung scharfkantiger schlanker Deltoflügel bei grossen Anstellwinkeln. Zeitscrift für Flugwissenschaften, Vol. 15, p 376 (1967)
2	E. C. Maskell J. Weber	On the aerodynamic design of slender wings. R.A.E. Report Aero 2610 (1958) A.R.C. 20610, J. Roy. Aero. Soc., Vol. 63, p 709 (1959)
3	J. C. Cooke	The laminar boundary layer on an inclined cone. A.R.C. R. & M. 3530 (1965)
4	J. C. Cooke	Approximate calculation of three-dimensional laminar boundary layers. A.R.C. R. & M. 3201 (1959)
5	M. G. Hall	A numerical method for calculating steady three-dimensional laminar boundary layers. R.A.E. Technical Report 67145 (1967) A.R.C. 29525

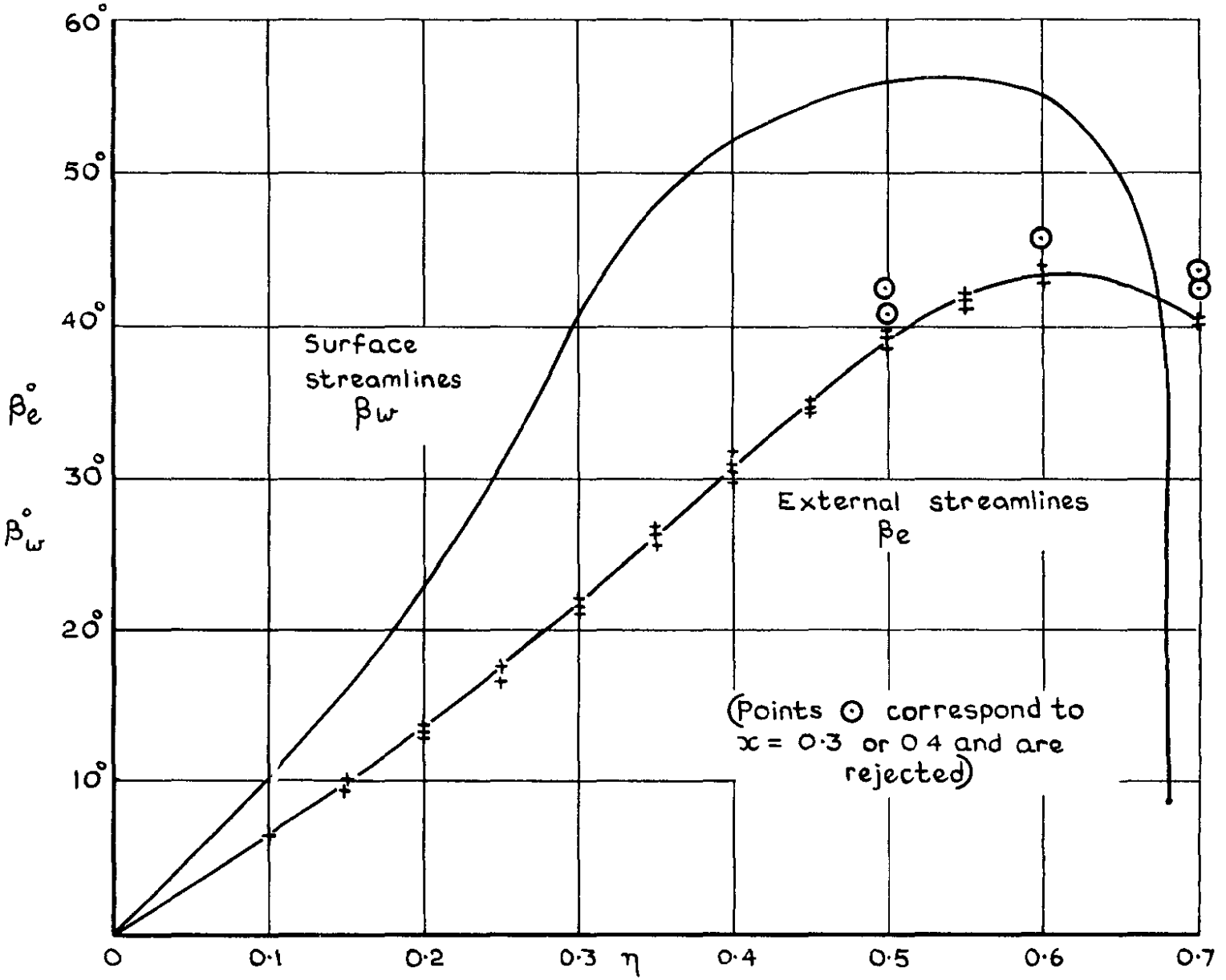

Fig. 1 Measured values of the angle between the centre line and external and surface streamlines

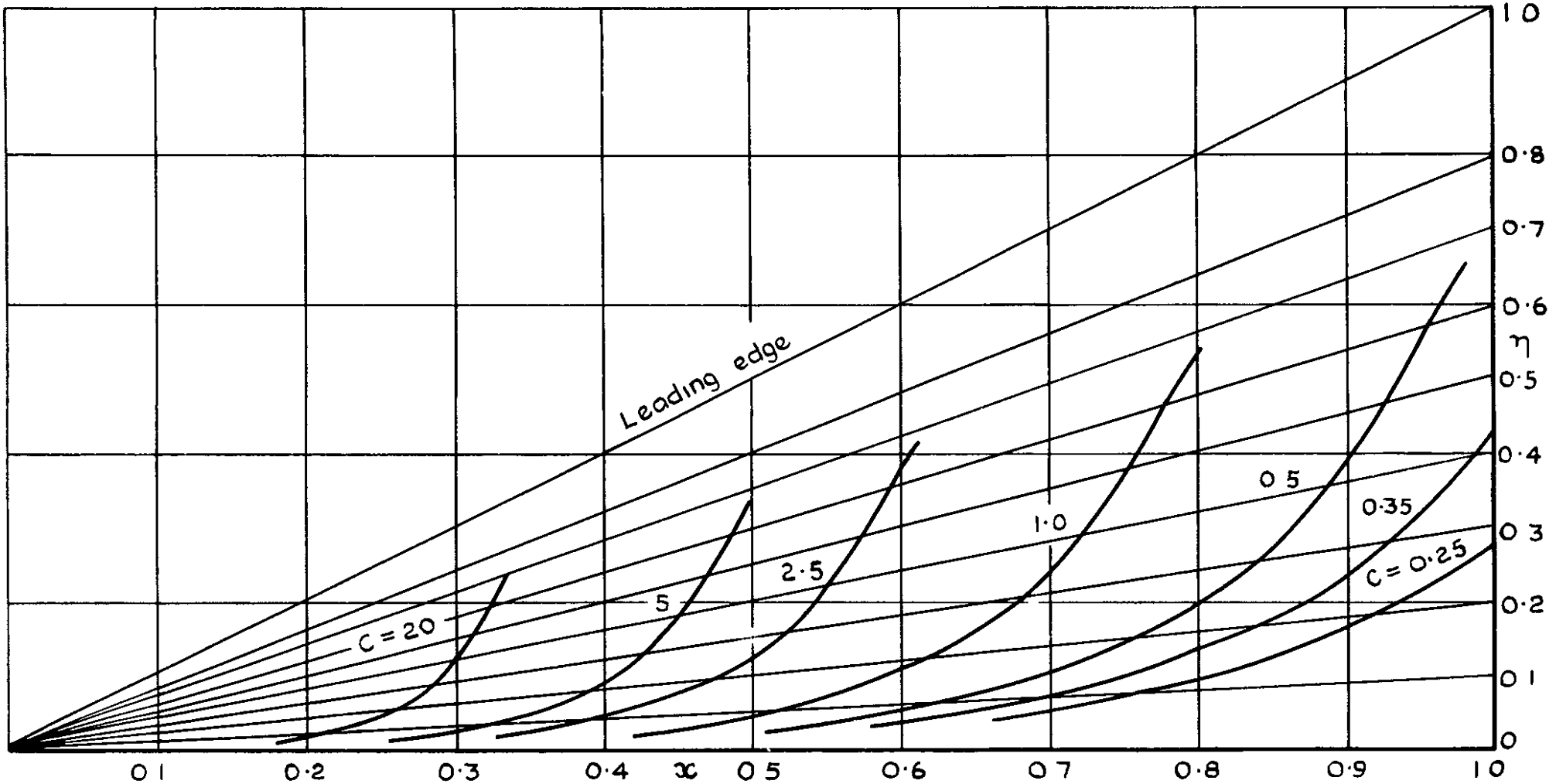

Fig.2 External streamlines. Vertical scale x 2

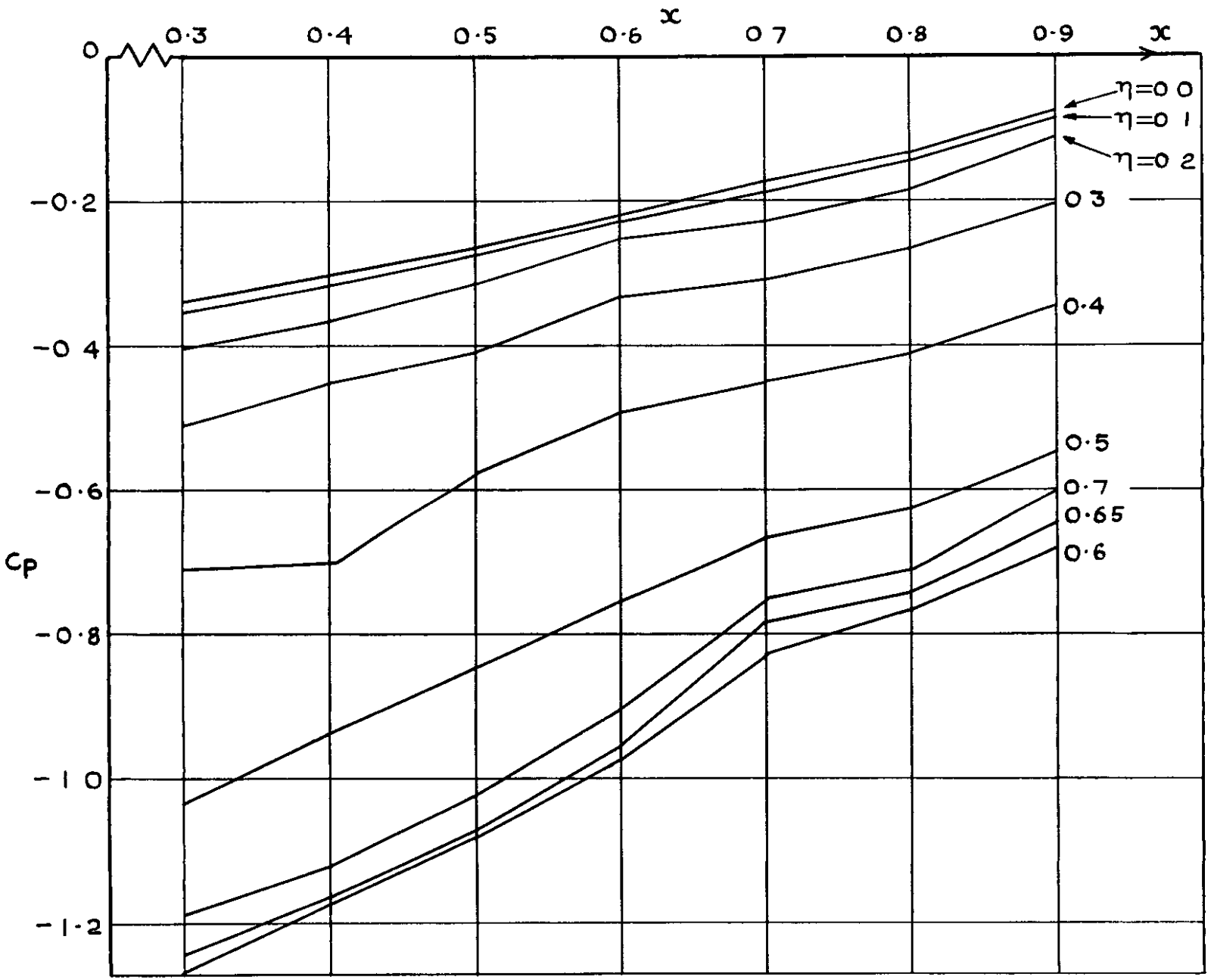

Fig 3 Measured pressure distribution. Upper surface

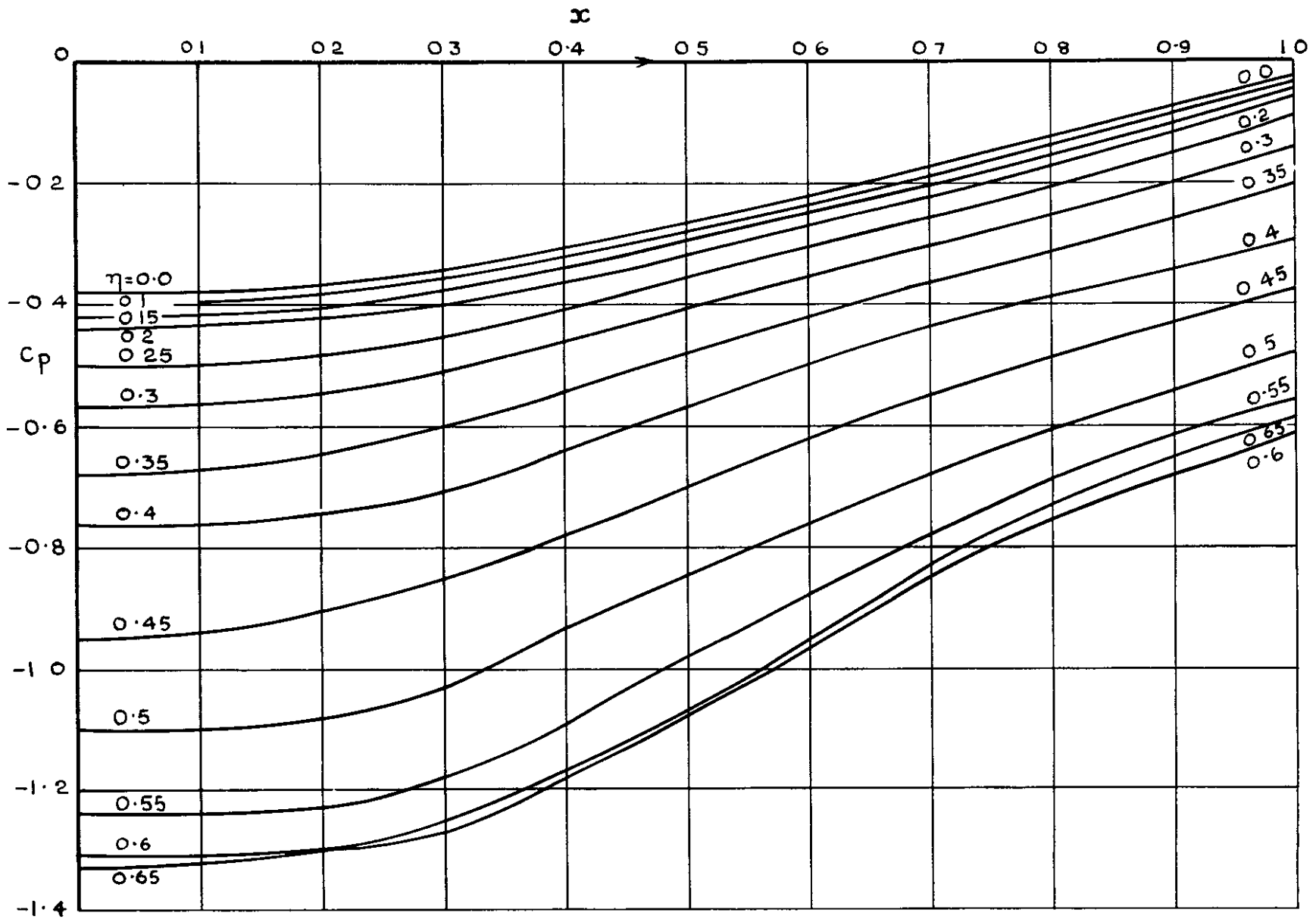

Fig 4 Smoothed pressure distribution used. Upper surface

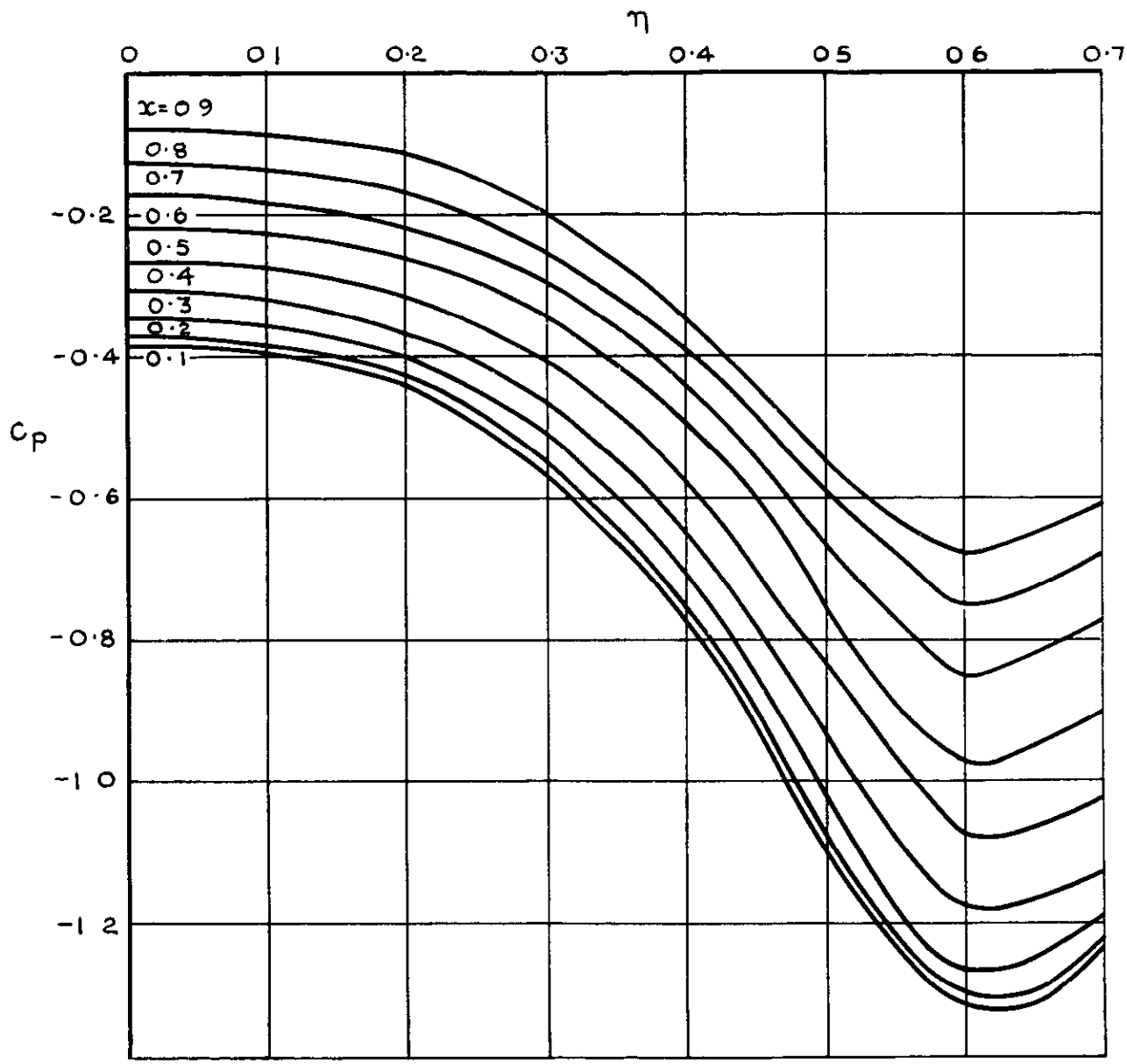

Fig.5 Smoothed pressure distribution used. Upper surface

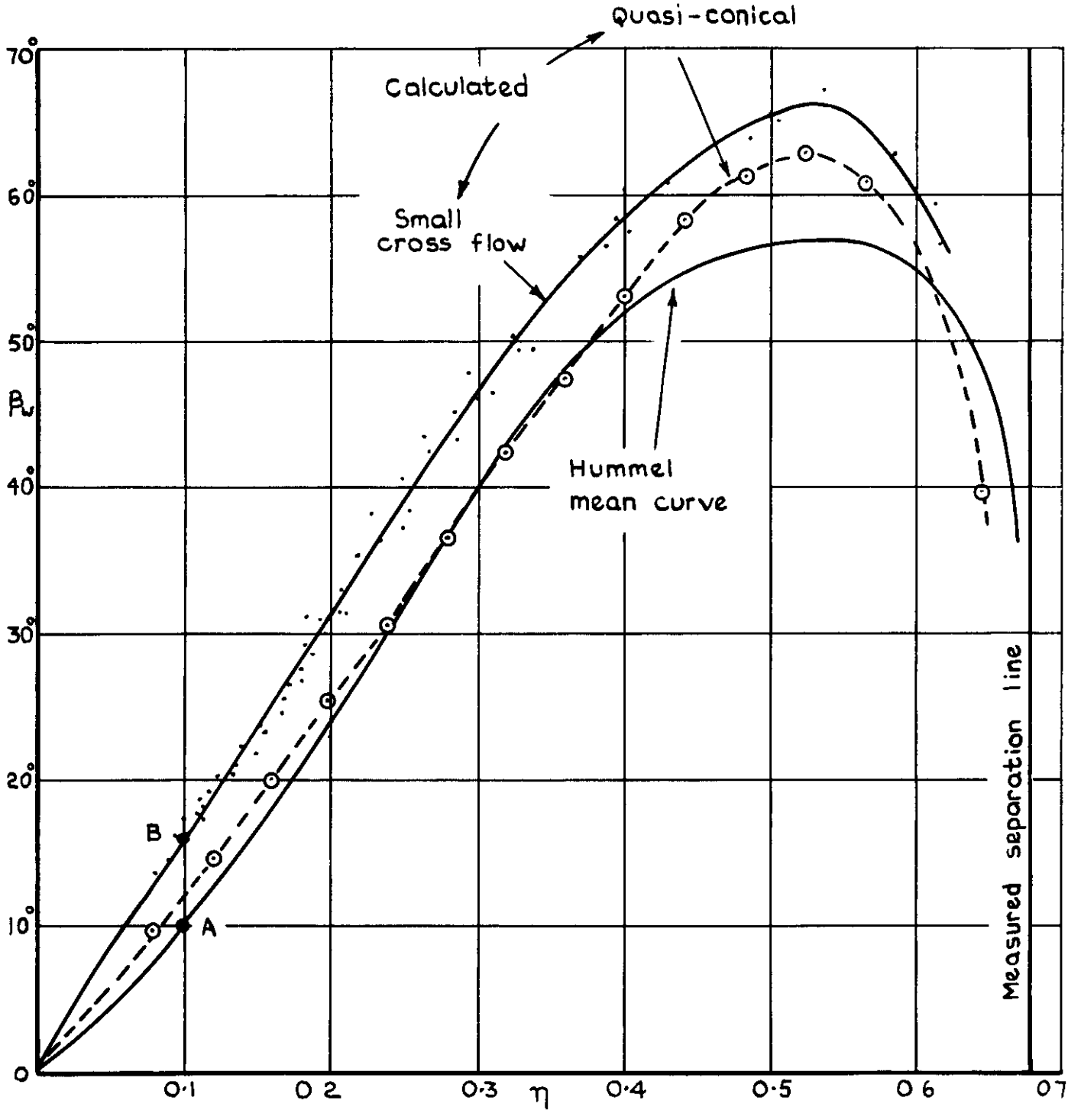

Fig. 6 Angle between limiting streamlines and centre line

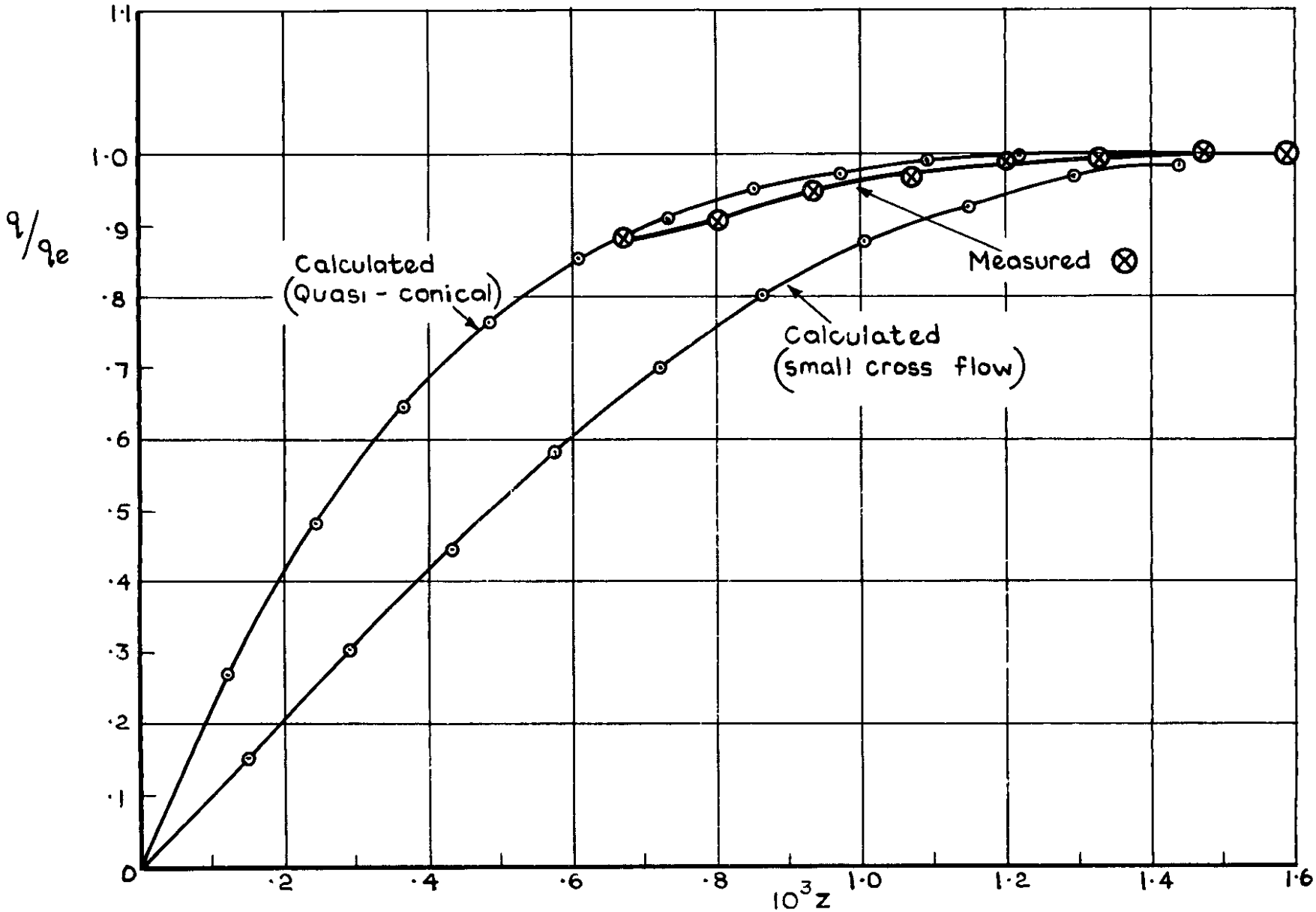

Fig 7 Measured and calculated resultant velocity at $x = 0.9$, $\eta = 0.2$

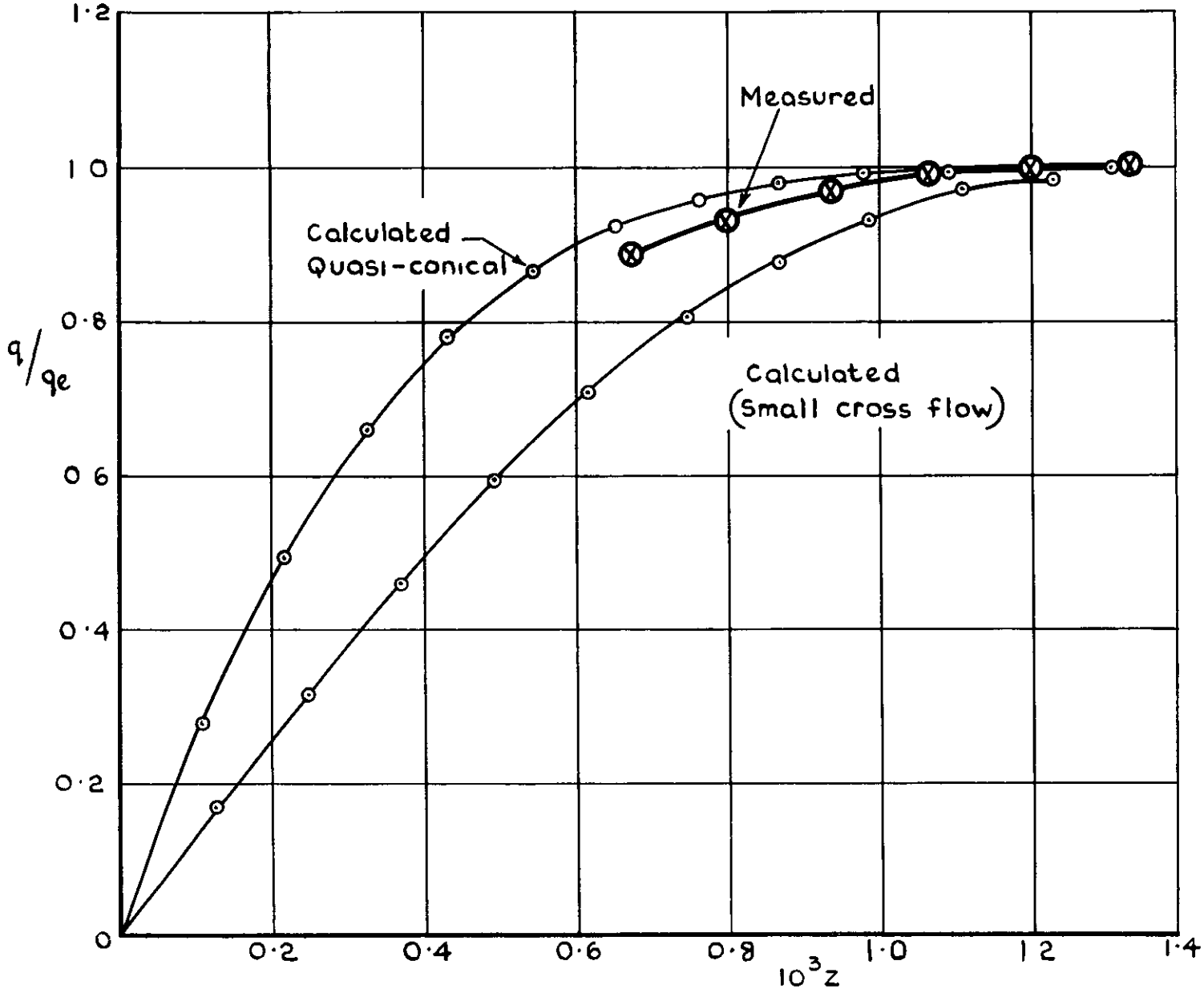

Fig.8 Measured and calculated resultant velocity at $x = 0.8$, $\eta = 0.25$

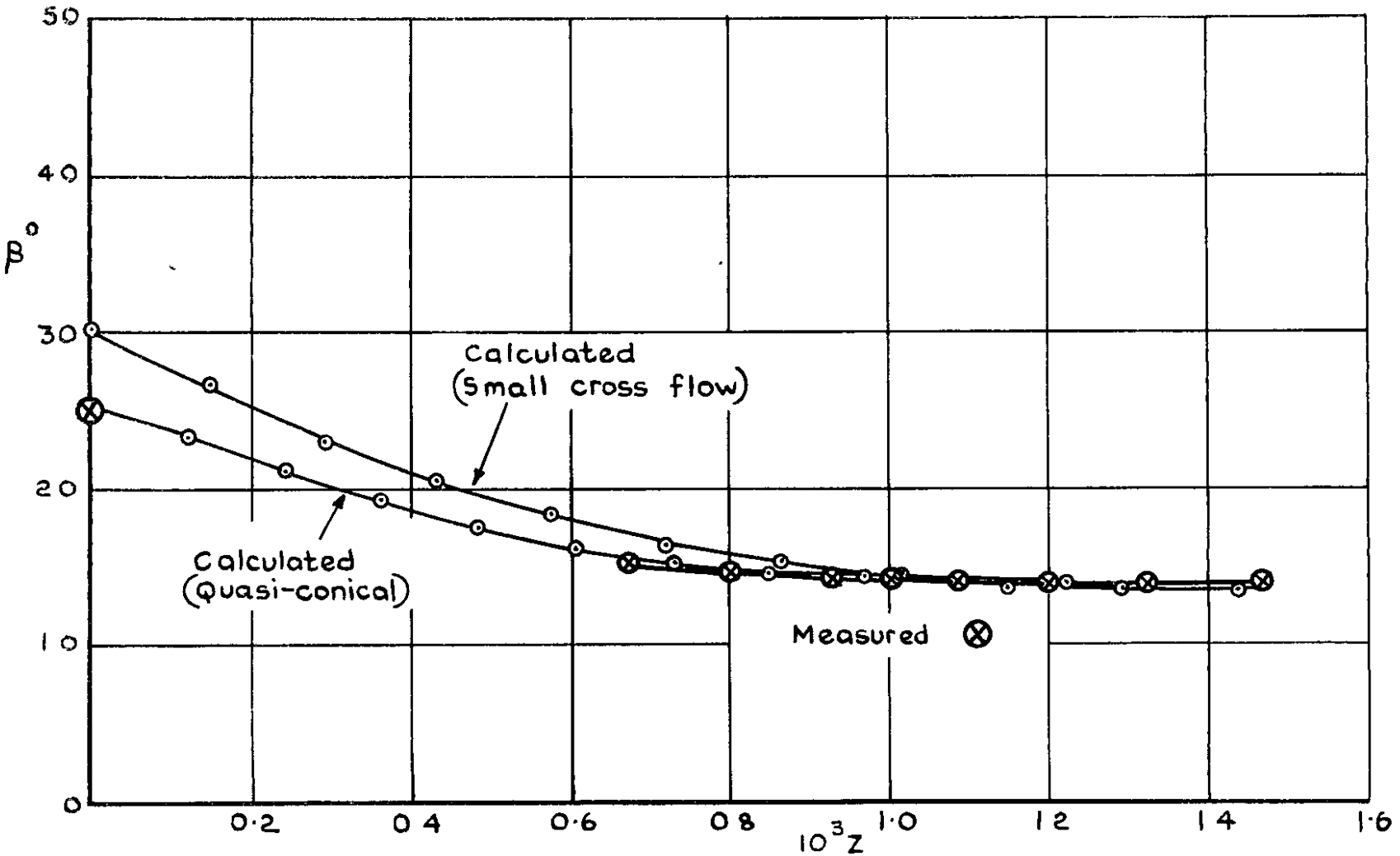

Fig. 9 Measured and calculated value of β at $x = 0.9$, $\eta = 0.2$

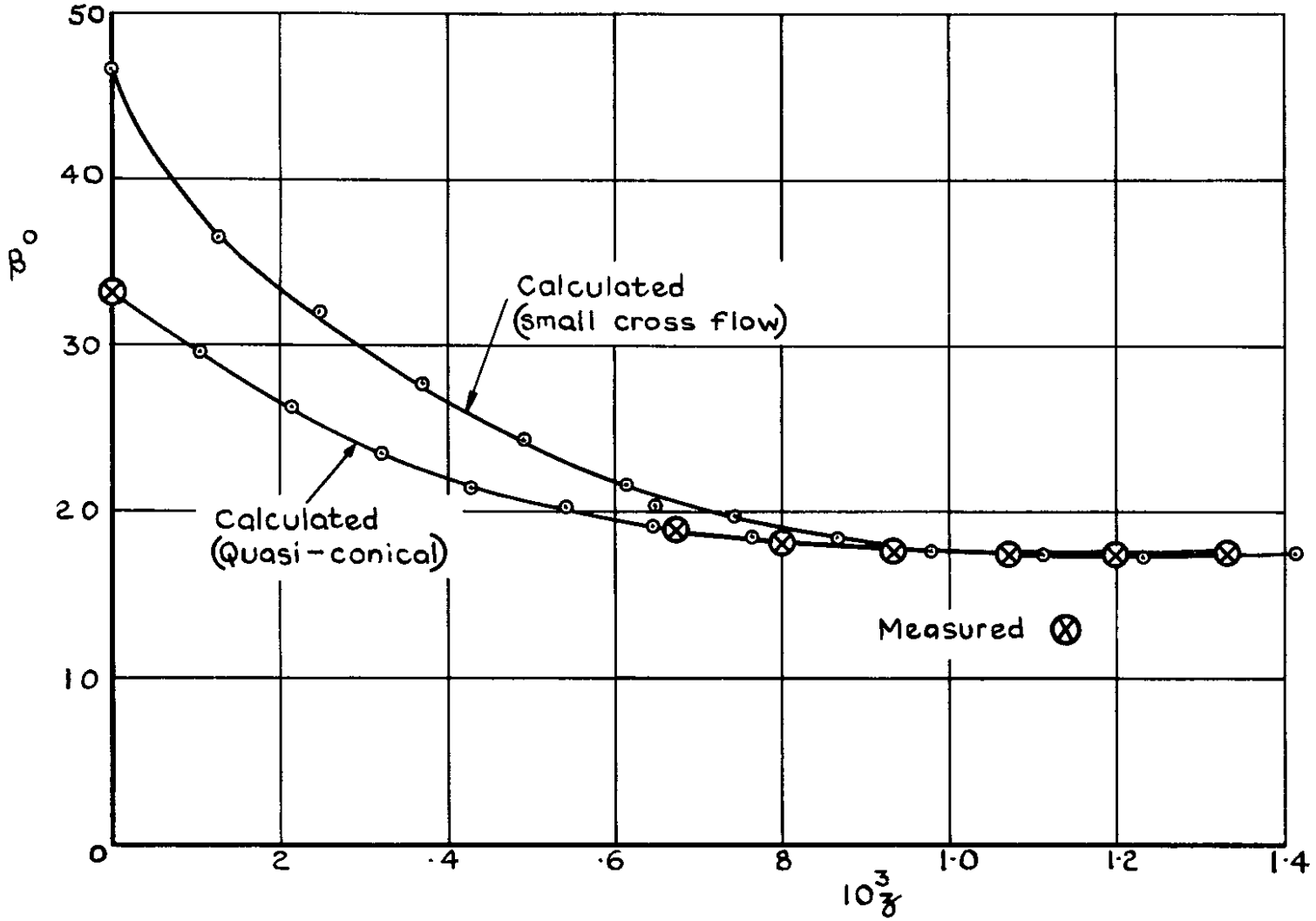

Fig.10 Measured and calculated value of β at $x = 0.8$ $\eta = 0.25$

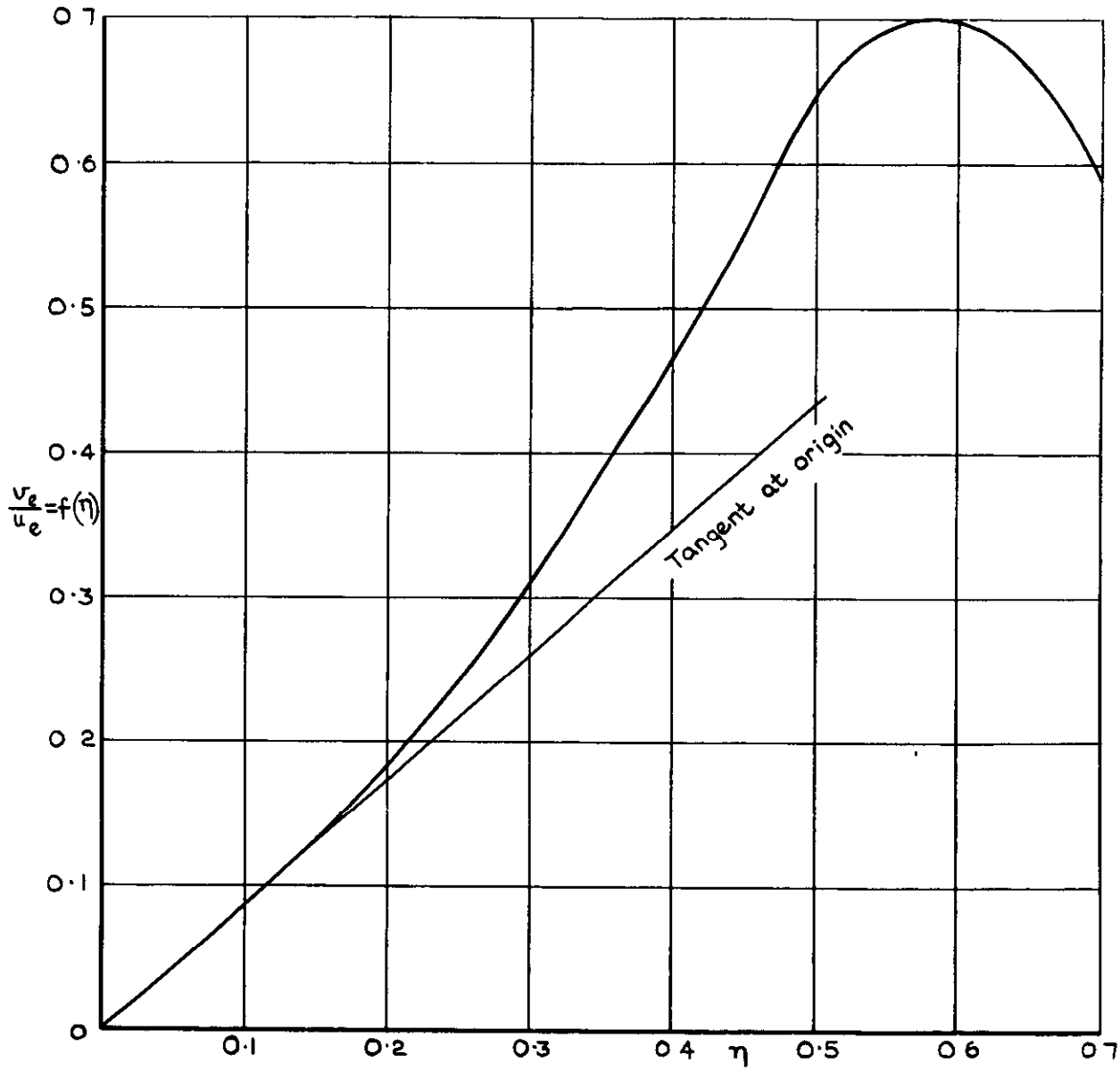

Fig.11 Value of $f(\eta)$

Printed in England for Her Majesty's Stationery Office by the Royal Aircraft Establishment, Farnborough. Dd.146915. K.4.

DETACHABLE ABSTRACT CARD

A.R.C. C.P. No. 1096
September 1967

Cooke, J. C.

LAMINAR BOUNDARY LAYER CALCULATIONS COMPARED WITH MEASUREMENTS BY HUMMEL

532.526.2 :
533.693.1 :
533.693.3 :
517.948.1 :
517.949.2 :
533.6.011.12

Calculations by an integral method assuming small cross-flow, and by a finite-difference method assuming the flow to be quasi-conical, are compared with measurements made available by Hummel (Technical University, Brunswick) on a highly swept delta wing at high incidence.

It is found that the small-cross-flow method gives a rough general picture of the flow but is inaccurate in the details, especially velocity profiles. For this problem the quasi-conical method is more accurate over most of the flow field and gives a much better representation of the velocity profiles.

A.R.C. C.P. No. 1096
September 1967

Cooke, J. C.

LAMINAR BOUNDARY LAYER CALCULATIONS COMPARED WITH MEASUREMENTS BY HUMMEL

532.526.2 :
533.693.1 :
533.693.3 :
517.948.1 :
517.949.2 :
533.6.011.12

Calculations by an integral method assuming small cross-flow, and by a finite-difference method assuming the flow to be quasi-conical, are compared with measurements made available by Hummel (Technical University, Brunswick) on a highly swept delta wing at high incidence.

It is found that the small-cross-flow method gives a rough general picture of the flow but is inaccurate in the details, especially velocity profiles. For this problem the quasi-conical method is more accurate over most of the flow field and gives a much better representation of the velocity profiles.

Published by
HER MAJESTY'S STATIONERY OFFICE

To be purchased from
49 High Holborn, London W.C 1
13a Castle Street, Edinburgh EH 2 3AR
109 St. Mary Street, Cardiff CF1 1JW
Brazennose Street, Manchester 2
50 Fairfax Street, Bristol BS1 3DE
258 Broad Street, Birmingham 1
7 Linenhall Street, Belfast BT2 8AY
or through any bookseller

C.P. No. 1096

SBN 11 470296 9